Methionyl-tRNA Synthetase Induced 3′-Terminal and Delocalized Conformational Transition in $tRNA^{fMet}$: Steady-State Fluorescence of tRNA with a Single Fluorophore†

Blair Q. Ferguson‡ and David C. H. Yang*

Department of Chemistry, Georgetown University, Washington, D.C. 20057

Received July 24, 1985

ABSTRACT: Five species of $tRNA^{fMet}$ labeled with a single fluorophore are prepared to analyze the conformational changes at the 3′-end, at dihydrouridine, and at thiouridine in $tRNA^{fMet}$ upon binding of methionyl-tRNA synthetase. The emission and excitation spectra, anisotropy, and solvent accessibility of the fluorophore in each of the modified $tRNA^{fMet}$'s are determined in the absence and presence of methionyl-tRNA synthetase. The results are consistent with the following. The probes at the 3′-end are in a nonpolar environment, mobile relative to the tRNA molecule, and fully exposed to the solvent. The probes at dihydrouridine are partially stacked over the neighboring bases, nearly immobile, and relatively inaccessible. The S8–C13 cross-linked product is rigid. Upon binding of methionyl-tRNA synthetase, the probes at the 3′-terminus become localized in a less polar environment, highly immobilized, and effectively shielded against solvent access, while the probes at dihydrouridine appear to be partially unstacked from the neighboring base and become slightly more accessible for solvent. Singlet–singlet energy transfer between the intrinsic protein fluorescence and the fluorophores in modified tRNA's was observed by sensitized emission for $tRNA^{fMet}$ modified at the 3′-end and for S8–C13 but not for $tRNA^{fMet}$'s modified at dihydrouridine. These results suggest that dihydrouridine in $tRNA^{fMet}$ is oriented away from methionyl-tRNA synthetase in the tRNA–enzyme complex.

The specific recognition of tRNA and cognate aminoacyl-tRNA synthetases has provided attractive model systems for studies of nucleic acid–protein interaction in general [for a review, see Schimmel & Söll (1979)]. The interaction of $tRNA^{fMet}$ and methionyl-tRNA synthetase appears to be a particularly useful system. The crystal structure of $tRNA^{fMet}$ has been resolved at 3.5 Å (Woo et al., 1980). The solution structure of $tRNA^{fMet}$ has been examined with high-resolution NMR (Crothers et al., 1974), nuclease mapping (Dube, 1973; Wrede et al., 1979), and singlet–singlet energy transfer (Yang & Söll, 1974). Methionyl-tRNA synthetase from *Escherichia coli* consists of two identical subunits of 76 000 daltons each (Blanquet et al., 1979). The crystal structure of trypsin-modified methionyl-tRNA synthetase (Cassio & Waller, 1974) has been resolved at 2.5 Å and shows a characteristic "nucleotide binding fold" (Risler et al., 1981; Zelwer et al., 1982). Partial amino acid sequence of methionyl-tRNA synthetase has been determined from the nucleotide sequence of the cloned gene (Barker et al., 1982).

Numerous studies of the interaction of $tRNA^{fMet}$ and methionyl-tRNA synthetase by chemical modification have elucidated the role of the nucleotide sequence [e.g., Schulman et al. (1983) and Schulman & Pelka (1977)]. It appears that some of the "discriminatory" nucleotides involved in recognition are scattered over the entire $tRNA^{fMet}$ molecules. Support of this notion has been obtained by comparison of nucleotide sequences of isoacceptors and photo-cross-linking (Ackerman et al., 1985; Rosa et al., 1979) and base substitution (Uemura et al., 1982). Studies of the relaxation kinetics (Krauss et al., 1976) suggest a critical role of the conformational changes of tRNA in the recognition process, and neutron scattering studies revealed significant conformational changes in $tRNA^{fMet}$ upon binding of methionyl-tRNA synthetase (Dessen et al., 1982).

We have sought to localize the conformational changes in $tRNA^{fMet}$ upon binding of methionyl-tRNA synthetase using fluorescence spectroscopy. In this paper, we define the conformational changes in tRNA in terms of the polarity of the local environment of the fluorophores, their rotational mobility, and solvent accessibility. The relative orientation of tRNA and synthetase is analyzed by the singlet–singlet energy transfer between the intrinsic protein fluorescence and the fluorophore in tRNA. A preliminary report of this study has appeared (Ferguson & Yang, 1981).

Materials and Methods

Materials. Dansylhydrazine and 5-[[[(iodoacetyl)-amino]ethyl]amino]naphthalene-1-sulfonic acid (1,5-IAEDANS) were obtained from Molecular Probes. Ethidium bromide, proflavin, fluoresceinyl isothiocyanate, hydrazine, and acrylamide were from Sigma. Acrylamide was recrystallized from ethyl acetate before use. Spectrophotometric-grade guanidine hydrochloride and dimethyl sulfoxide were obtained from Heico and Aldrich, respectively. Sodium cyanoborohydride was from Aldrich. Cibacron blue F3GA was obtained from Pierce. All other chemicals were reagent-grade or the purest form available from standard sources.

Aminoacylation Assay. The extent of aminoacylation of $tRNA^{fMet}$ with [^{14}C]methionine was assayed as described (Johnson et al., 1979). The assay mixture contained in a total volume of 50–100 μL 50 mM Tris-HCl[1] (pH 7.5 at 37 °C),

†This work was supported by grants from NIH (GM-25848) and NSF (81-10818).

*Address correspondence to this author.

‡Present address: Dupont Experimental Station, Wilmington, DE 19898.

0006-2960/86/0425-0529$01.50/0

6 mM $MgCl_2$, 4 mM dithioerythritol, 2.5 mM ATP, 40 μM [^{14}C]methionine (50 mCi/mmol) (New England Nuclear), and 50 A_{260}/mL *E. coli* MRE 600 $tRNA^{fMet}$ (Boehringer Mannheim).

Preparation and Properties of E. coli Methionyl-tRNA Synthetase. Methionyl-tRNA synthetase (MetRS) was purified from *E. coli* K12 (Grain Processing Co.) according to the procedure of Lemoine et al. (1968), with some modifications. Methionyl-tRNA synthetase obtained by this procedure was further purified by a Cibacron F3GA–Sepharose chromatography step, as described below. The purified MetRS was greater than 95% pure, as judged by polyacrylamide gel electrophoresis in the presence of sodium dodecyl sulfate (SDS). The specific activity of the purified MetRS was 11 units/mg, where 1 unit of enzyme is defined as the amount of enzyme that will form 1 μmol of aminoacyl-tRNA in 10 min at 37 °C.

The native molecular weight of purified MetRS, as determined by Sephadex G-200 chromatography, is about 170 000, which is in agreement with the value reported previously (Heinrikson & Hartley, 1967; Lemoine et al., 1968). The subunit molecular weight of MetRS was determined by SDS–polyacrylamide gel electrophoresis (Laemmli, 1970) to be 76 000.

F3GA–Sepharose was prepared by covalently coupling Cibacron blue F3GA to Sepharose 4B, according to the procedure of Bohme et al. (1972). The sample, containing 10 mM $MgCl_2$, was loaded to a F3GA–Sepharose column preequilibrated with a buffer containing 20 mM imidazole hydrochloride (pH 7.5), 20 mM 2-mercaptoethanol, and 5 mM $MgCl_2$. The column was washed extensively with the equilibrium buffer, containing 0.3 M KCl. MetRS was eluted by washing the column with a buffer containing 20 mM imidazole hydrochloride (pH 7.5) and 2-mercaptoethanol. The F3GA–Sepharose chromatography step was found to clearly resolve proteins that had copurified with MetRS through the conventional purification procedure (Lemoine et al., 1968).

Covalent Attachment of Fluorescence Probes. $tRNA^{fMet}$ (3′-DNS) was prepared by reaction of periodate oxidized $tRNA^{fMet}$ with dansylhydrazine in the presence of sodium cyanoborohydride according to Wells & Cantor (1977). $tRNA^{fMet}$(3′-Flc) was prepared by reaction of periodate-oxidized $tRNA^{fMet}$ with fluoresceinyl thiosemicarbazide (Wells & Cantor, 1980). $tRNA^{fMet}$(8–13), which contains a cross-link between S8 and C13, was prepared by irradiation of $tRNA^{fMet}$ at 335 nm with an Oriel 500-W mercury lamp followed by reduction with $NaBH_4$ (Favre et al., 1971). $tRNA^{fMet}$(D-Etd) and $tRNA^{fMet}$(D-PF) were prepared by replacement of D20 with ethidium and proflavin, respectively, followed by $NaCNBH_3$ reduction according to Wintermeyer & Zachau (1979). Unreacted dyes were removed by four to six consecutive ethanol-precipitation steps until no free dye was detectable by thin-layer chromatography. The extent of labeling was determined from the absorbance at the absorption maximum, by using $\epsilon_{462nm} = 3.3 \times 10^4$ M^{-1} cm^{-1} for proflavin (Wintermeyer & Zachau, 1979), $\epsilon_{386nm} = 1.6 \times 10^4$ M^{-1} cm^{-1} for the 8–13 cross-link (Bergstrom & Leonard, 1972), $\epsilon_{515nm} = 5.3 \times 10^3$ M^{-1} cm^{-1} for the labeled ethidium (Hudson & Jacobs, 1975; Wintermeyer & Zachau, 1979), and $\epsilon_{493nm} = 6.9 \times 10^4$ M^{-1} cm^{-1} for fluorescein (Odom et al., 1980). The extent of labeling of $tRNA^{fMet}$(3′-DNS) was determined from the emission in 98% Me_2SO with dansylhydrazine in 98% Me_2SO as standard, since the absorbance is low. These labeling procedures were well characterized and were previously shown to be specific for the 3′-end (Wells & Cantor, 1977, 1980), the 8–13 cross-link (Favre et al., 1971), and dihydrouracil (Wintermeyer & Zachu, 1979). No sequence analyses were made for the present investigation. Care was taken to protect samples from light throughout.

Steady-State Fluorescence. Steady-state fluorescence measurements were performed on a Hitachi Perkin-Elmer Model MPF-2A fluorometer, with a thermostated cell compartment at 20 °C. All fluorescence measurements were made in 0.4 × 0.4 cm^2 microcuvettes. Fluorescence titrations were performed by adding 1-μL aliquotes in an initial volume of 250 μL with a 5-μL capacity Hamilton syringe. Fluorescence experiments were carried out in a standard buffer containing 20 mM imidazole hydrochloride (pH 7.5), 10 mM $MgCl_2$, and 10 mM 2-mercaptoethanol. The 2-mercaptoethanol was added just prior to use of the buffer. All fluorescence titration data were corrected for dilution of the sample in the course of the titration. The contribution to the observed emission intensity of each individual component in a multicomponent sample was corrected by determining parallel control measurements. For any particular fluorescence titration, all control experiments were performed on the same day with the same solutions and fluorometer settings. The effects of inner filter absorption were corrected by performing parallel control experiments. Quenching of fluorescence due to self-absorbance of exciting or emitting light was detected by the addition of an individual fluorescent component to standard buffer.

The relative quantum yield of the various fluorescent probes in standard buffer was determined as described by Cantley & Hammes (1976):

$$\Phi_1/\Phi_2 = (F_1/F_2)(A_2/A_1)(1 - r_1/4)$$

where Φ is the quantum yield, F is the area of the corrected emission spectrum, A is the absorbance at the exciting wavelength, and r is the emission anisotropy. The term $1 - r_1/4$ is a correction for polarized emission (Shinitzky, 1972). The fluorescence emission spectra were corrected for the wavelength dependence of the detection system sensitivity with correction factors determined by comparison of the observed quinine sulfate emission spectrum with the corrected spectrum (Scott et al., 1970).

Fluorescence Titration of the Intrinsic Fluorescence of MetRS. The interaction of MetRS with $tRNA^{fMet}$ is accompanied by a large decrease in the MetRS tryptophan emission intensity (Bruton & Hartley, 1970; Blanquet et al., 1973). Tryptophan quenching was monitored at 330 nm with an excitation wavelength at 295 nm. The MetRS tryptophan emission was corrected for dilution and inner filter absorption.

The functions used to fit the data were calculated with (Pachmann et al., 1973; Engel, 1974)

$$\alpha = \frac{\Delta F}{\Delta F_{max}} = \frac{(nE_0 + x_0 + K) - [(nE_0 + x_0 + K)^2 - 4nE_0x_0]^{1/2}}{2nE_0} \quad (1)$$

where

$$\alpha = \frac{\Delta F}{\Delta F_{max}} = \frac{F_0 - F}{F_0 - F_{max}} = \frac{x_b}{nE_0}$$

F_0, F, and F_{max} are the MetRS tryptophan emission intensities in the absence of $tRNA^{fMet}$, in the presence of limiting $tRNA^{fMet}$, and in the presence of saturating $tRNA^{fMet}$, respectively. x_0 is the total concentration of $tRNA^{fMet}$, x_b is the concentration of bound $tRNA^{fMet}$, n is the number of binding

[1] Abbreviations: DNS, (dimethylamino)naphthalenesulfonyl; Flc, fluorescein; PF, proflavin; Etd, ethidium; MetRS, methionyl-tRNA synthetase; Tris-HCl, tris(hydroxymethyl)aminomethane hydrochloride.

sites per MetRS molecule, and E_0 is the total MetRS concentration.

Fluorescence Titration of the Fluorophore in Modified tRNA. Fluorescence titration data, in which MetRS was added to fluorescent-labeled tRNA^{fMet}, were fit according to

$$\alpha = \frac{(x_0 + nE_0 + K) - [(x_0 + nE_0 + K)^2 - (4x_0nE_0)]^{1/2}}{2x_0} \quad (2)$$

$$\alpha = \frac{\Delta F}{\Delta F_{max}} = \frac{F - F_0}{F_{max} - F_0} = \frac{x_b}{x_0}$$

F_0, F, and F_{max} are the emission intensities of the labeled tRNA^{fMet} in the absence and in the presence of a limiting concentration and in the presence of saturating concentration of methionyl-tRNA synthetase, respectively; x_0 is the total concentration of tRNA^{fMet}, and x_b is the concentration of bound tRNA^{fMet}. K is the equilibrium dissociation constant, n is the number of binding sites per MetRS molecule, and E_0 is the total MetRS concentration. K is solved from the above equation, mass conservation, and the Scatchard relation for the binding of a ligand at n identical, independent sites. Fits of the fluorescence titration data, according to eq 2, were obtained by nonlinear regression methods. For all fluorescence titrations, the data were shown to deviate randomly from the theoretical fit by plotting the residuals vs. either F or E_0.

Steady-State Fluorescence Anisotropy. The emission anisotropy, r, was measured according to the definition

$$r = \frac{F_{VV} - F_{VH}(F_{HV}/F_{HH})}{F_{VV} + 2F_{VH}(F_{HV}/F_{HH})}$$

where F_{12} is an emission intensity and the subscripts 1 and 2 indicate the position of the excitation and emission polarizers, respectively. The polarizers are in either the vertical, V, or horizontal, H, position.

The anisotropy of fluorophore will depend, among other things, on the rotational diffusion of the fluorophore (Cantor & Tao, 1971; Yguerabide, 1972; Wahl, 1975; Dale & Eisenger, 1975). For a rigid spherical molecule, the rotational motion is isotropic, and the decay of anisotropy is given by

$$r(t) = r(0)e^{-t/\phi}$$

where ϕ is the rotational relaxation time. The steady-state anisotropy, r, for a rigid sphere is given by

$$1/r = 1/r_0 + (1/r_0)(\tau/\phi) \quad (3)$$

where r_0 is the limiting anisotropy in the absence of molecular rotations and τ is the lifetime of the excited singlet state.

The steady-state anisotropy is measured as a function of solvent viscosity, at constant T and τ, and plotted as $1/r$ vs. $1/\eta$ to obtain the limiting anisotropy. The limiting anisotropy was determined as the intercept of a linear Perrin plot, and an apparent rotational relaxation time was determined from the slope of a linear Perrin plot, using eq 3.

The solvent viscosity of a sample was varied, at 20 °C, by decreasing the sucrose concentration by dilution with standard buffer or by increasing the sucrose concentration by dilution with standard buffer containing 64% sucrose. The viscosity values for sucrose in water at 20 °C were taken from the *Handbook of Biochemistry* (Fasman, 1975). It was verified, in all experiments, that the emission spectra of the fluorophore were not shifted, as the sucrose concentration was varied.

Fluorescence Lifetime Measurements. Fluorescence lifetimes were determined by the single-photon counting technique (Yguerabide, 1972) by using an Ortec Model 9200 nanosecond fluorescence spectrometer equipped with an RCA 8850 photomultiplier tube. Excitation pulses were generated by an Ortec Model 9352 light pulser operated with air at close to ambient pressure. The decay data were accumulated and analyzed by using an Ino-tech multichannel analyzer interfaced to a Data General Nova 3 computer. The excitation and emission wavelength bands were selected with the appropriate Corning glass filters. Lifetime measurements were made in 0.4 × 0.4 cm^2 cuvettes placed in a thermostated cell compartment at 20 °C. Slit widths were controlled to maintain an emission counting frequency of <5%. The lamp pulse (pulse half-width = 2.5 ns) was collected by scattering light from a solution of Ludox (Du Pont) with the excitation filter removed. The decay data were deconvoluted with the lamp pulse and analyzed in terms of one or two fluorescence lifetimes by the method of moments (Yguerabide, 1972).

Dynamic Quenching. Dynamic quenching of a single fluorescent component is described by the Stern–Volmer equation (Stern & Volmer, 1919):

$$\frac{\tau_0}{\tau} = \frac{F_0}{F} = 1 + k_q\tau_0[Q] = 1 + K_a[Q] \quad (4)$$

where τ_0 and τ are the fluorescence lifetimes in the absence and presence of quencher, F_0 and F are the fluorescence intensities in the absence and presence of quencher, k_q is the bimolecular quenching rate constant, and [Q] is the quencher concentration. Corrections were made for dilution and quencher emission; 8 M acrylamide and 5 M KI were used for quenching experiments (Eftink & Ghiron, 1977). The presence of the quencher did not shift the excitation and emission spectra of the fluorophore in the cases reported here.

Energy Transfer. The efficiency of energy transfer, E, between a single donor and acceptor pair is related to the distance separating the pair, R, by eq 5, where R_0 is the

$$E = R_0^6/(R^6 + R_0^6) \quad (5)$$

distance at which transfer efficiency is 0.50 (Forster, 1948). The energy-transfer efficiency measured by sensitized acceptor emission, E_A, was calculated as follows (Fairclough & Cantor, 1978; Berman et al., 1980):

$$E_A = \frac{A^A_{DA}(\lambda_D)}{A^D_{DA}(\lambda_D)}\left[\frac{F^A_{DA}(\lambda_D,\lambda_A)}{F_A(\lambda_D,\lambda_A)} - 1\right]$$

where $A^A_{DA}(\lambda_D)$ and $A^D_{DA}(\lambda_D)$ are the absorbance of the tRNA–enzyme complex at the wavelength of the absorbance maximum of the donor for the acceptor and donor, respectively, and $F^A_{DA}(\lambda_D,\lambda_A)$ and $F_A(\lambda_D,\lambda_A)$ are the fluorescence intensity observed at the donor's excitation maximum wavelength and the acceptor's emission maximum for labeled tRNA–enzyme complex and labeled tRNA alone, respectively. F^A_{DA} is corrected for the contribution of donor emission according to Fairclough & Cantor (1978). The calculated transfer efficiency was corrected for the labeling stoichiometry of the fluorophore in modified tRNA. The observed apparent transfer efficiency was below 3% in all cases.

Results

Modification of tRNA^{fMet}. The stoichiometry of the label in modified tRNA's and their methionine acceptor activity are shown in Table I. These results are in accordance with those previously reported for each of the modification procedures.

All five species of modified tRNA^{fMet} retained the capability of binding to native methionyl-tRNA synthetase. As shown in Figure 1, the protein fluorescence is quenched about 40% by native tRNA^{fMet} as well as by all modified tRNA^{fMet}'s. Under the conditions used (10 mM Mg^{2+}), the dimeric methionyl-tRNA synthetase showed strong negative cooper-

Table I: Properties of $tRNA^{fMet}$ with Single Covalently Attached Fluorophore

	labeling stoichiometry (mol of label/ mol of tRNA)	app dissoc const, K (μM)[a]	rel intrinsic fluorescence, $(F/F_0)_{max}$[a]	max extent of aminoacylation (nmol of methionine/ A_{260} unit)	Michaelis const or inhibition const, K_M or K_I (μM)	V_{max} (pmol min^{-1} $nmol^{-1}$ at 30 °C)
$tRNA^{fMet}$		0.22	0.52	1.5	2.3	9.3
$tRNA^{fMet}$(3′-DNS)	0.70	0.41	0.54	0.0	3.0	
$tRNA^{fMet}$(3′-Flc)	0.98	0.14	0.48	0.0	1.4	
$tRNA^{fMet}$(8–13)	0.92	0.46	0.52	1.5	3.6	2.5
$tRNA^{fMet}$(D-Etd)	0.75	0.40	0.55	1.1	1.9	1.8
$tRNA^{fMet}$(D-PF)	0.65	0.31	0.62	0.75	1.9	2.6

[a] Apparent dissociation constant is calculated according to eq 1 on the basis of the data in Figure 1. Relative intrinsic fluorescence refers to the ratio of the intrinsic protein fluorescence in the presence and absence of a saturating amount of $tRNA^{fMet}$. Michaelis constants (K_M) and maximal velocity (V_{max}) are obtained from the Eddie–Hofstie plots of steady-state kinetic measurements of the rates of aminoacylation at varying concentrations of tRNA and saturating concentrations of ATP and methionine. The inhibition constants are obtained from the Dixon plot by using varying concentrations of 3′-labeled tRNA and constant fixed concentration of $tRNA^{fMet}$ with saturating concentration of ATP and methionine. The aminoacylation assay mixture contained 50 mM Tris-HCl (pH 7.5). The titration buffer contained 20 mM imidazole (pH 7.5). The correlation coefficients in the plots for the determination of dissociation constants and Michaelis constants are better than 0.98 in all cases.

ativity and binds one $tRNA^{fMet}$ per each dimer (Blanquet, 1979). The dissociation constants of modified $tRNA^{fMet}$ calculated according to eq 1 are very close to that of unmodified $tRNA^{fMet}$ (Table I). Similar dissociation constants were also determined by monitoring the changes of fluorescence of some of the modified tRNAs upon binding of methionyl-tRNA synthetase.

The Michaelis–Menten constants for native and modified $tRNA^{fMet}$ were determined from initial velocity measurements of aminoacylation of tRNA. As shown in Table I, the modified $tRNA^{fMet}$ showed similar Michaelis–Menten constants as that of native $tRNA^{fMet}$. However, appreciable decreases of V_{max}'s were observed for modified $tRNA^{fMet}$ (Table I). Modification at the 3′-end of tRNA abolished aminoacylation activity; the inhibition constants were thus determined with a Dixon plot (1/velocity vs. concentration of inhibitor) for comparison. As shown in Table I, the inhibition constants of 3′-end modified $tRNA^{fMet}$ are similar to the Michaelis–Menten constants of native tRNA. The Michaelis–Menten and inhibition constants are significantly greater than the apparent dissociation constants from fluorescence titration curves due to the higher ionic strength in the assay mixture than that in the standard buffer for fluorescence measurements.

Although some of the modified $tRNA^{fMet}$ species appear to have lower affinity than native $tRNA^{fMet}$ for methionyl-tRNA synthetase, the affinity is significantly higher than those for noncognate tRNA, including $tRNA^{Phe}$, $tRNA^{Val}$, $tRNA^{Glu}$, and $tRNA^{Tyr}$ (Figure 1). It appears that modified $tRNA^{fMet}$'s are capable of binding methionyl-tRNA synthetase properly and sufficiently maintain the native structure of $tRNA^{fMet}$ to induce the conformational transition of methionyl-tRNA synthetase.

Interaction of $tRNA^{fMet}$(3′-Flc) with Methionyl-tRNA Synthetase. The apparent dissociation constant suggests that $tRNA^{fMet}$(3′-Flc) shows higher affinity for methionyl-tRNA synthetase than unmodified $tRNA^{fMet}$. The extent of quenching by $tRNA^{fMet}$(3′-Flc) approaches 53%, as compared to 48% for unmodified $tRNA^{fMet}$. The higher affinity and extent of quenching may reflect that the fluorescein moiety in $tRNA^{fMet}$(3′-Flc) interacts with the active site of methionyl-tRNA synthetase.

The emission intensity of fluorescein in $tRNA^{fMet}$(3′-Flc) is quenched by 42% in the presence of an excess amount of methionyl-tRNA synthetase. As shown in Figure 2, the Scatchard plot of the fluorescence titration indicates that there is one tRNA binding site in the dimeric methionyl-tRNA synthetase corresponding to a dissociation constant of 0.10 μM. When the Scatchard plot was analyzed according to a model of two independent, nonidentical sites, as formulated by Klotz & Hunston (1971), the high-affinity site exhibits at least 10-fold higher affinity toward methionyl-tRNA synthetase than the low-affinity site. This is in accordance with previously observed negative cooperativity of methionyl-tRNA synthetase from *E. coli* (Blanquet et al., 1979).

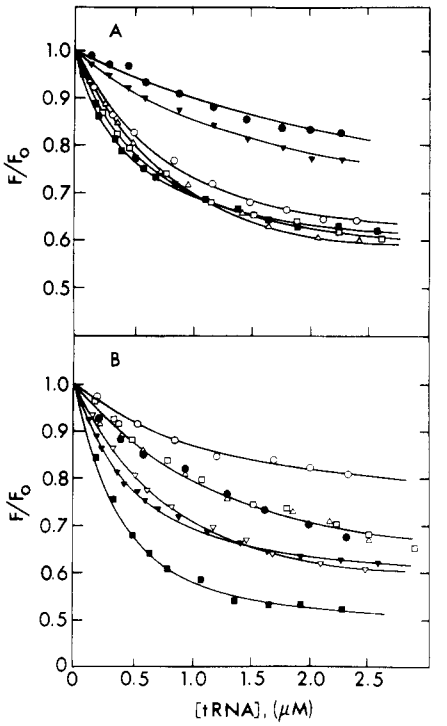

FIGURE 1: Intrinsic protein fluorescence titration of methionyl-tRNA synthetase (A) with native $tRNA^{fMet}$ (■), $tRNA^{fMet}$(D-PF) (○), $tRNA^{fMet}$(D-EB) (□), $tRNA^{fMet}$(8–13) (△), and noncognate $tRNA^{Glu}$ (▼) and $tRNA^{Val}$ (●) and (B) with native $tRNA^{fMet}$ (▼), $tRNA^{fMet}$(3′-Flc) (■), $tRNA^{fMet}$(3′-DNS) (▽), $tRNA^{Phe}$ (□), $tRNA^{Phe}$(3′-Flc) (△), $tRNA^{Phe}$(3′-DNS) (●), and $tRNA^{Tyr}$ (○). The concentration of methionyl-tRNA synthetase is 0.42 μM, except for that for $tRNA^{fMet}$(D-PF) which is 0.66 μM. Fluorescence intensity at 330 nm with excitation at 290 nm was monitored. All titrations are carried out in the standard buffer at 20 °C. Apparent dissociation constants fitting the data and eq 1 are shown in Table I.

The excitation and emission maxima of $tRNA^{fMet}$ (3′-Flc) are both red-shifted by 5 nm upon its binding of methionyl-tRNA synthetase. The excitation and emission spectral maxima for fluorescein are similarly red-shifted, as the concentration of ethanol increases. Thus, the 3′-Flc appears to become localized in a less polar environment. The fluorescence intensity of fluorescein, however, does not change significantly as the concentration of ethanol increases. When the emission lifetime of $tRNA^{fMet}$(3′-Flc) was determined by a single-

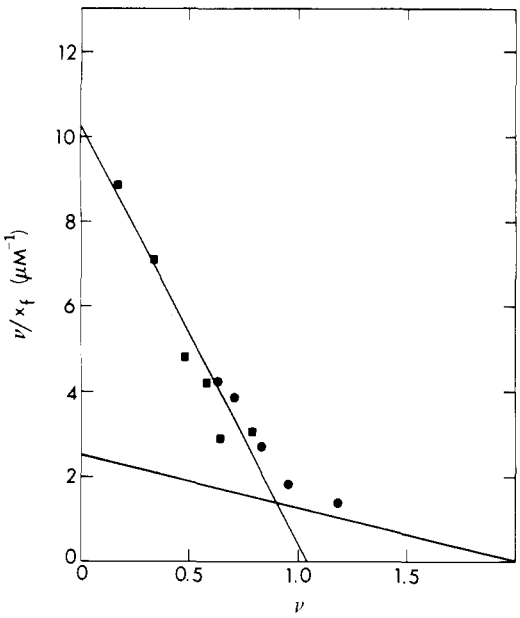

FIGURE 2: Scatchard plot of titration of the fluorescence of the fluorophore in tRNA^{fMet}(3′-Flc) with methionyl-tRNA synthetase. Two sets of titration were carried out. In the first set, aliquots of methionyl-tRNA synthetase are added to tRNA^{fMet}(3′-Flc) (■) and in the second set aliquots of tRNA^{fMet}(3′-Flc) are added to methionyl-tRNA synthetase (●). In the latter case, the changes in fluorescence intensity are obtained by the procedure described by Fairclough & Cantor (1979). Formalism of Klotz & Hunston (1971) was applied to fit the data for two independent binding sites. The calculated dissociation constants are $K_1 = 0.1$ μM and $K_2 > 1.7$ μM. The solid lines are the limiting slopes and intercepts for the fitted parameters.

photon counting method, both free and methionyl-tRNA synthetase bound tRNA^{fMet}(3′-Flc) showed an emission lifetime of 3.6 ns. These results suggest that static quenching dominates the quenching process of tRNA^{fMet}(3′-Flc) by methionyl-tRNA synthetase. Since fluorescein emission is known to decrease at acidic pH (Mercola et al., 1972), fluorescein in tRNA^{fMet}(3′-Flc) may be localized in a relatively more acidic environment in addition to a less polar environment upon binding of methionyl-tRNA synthetase.

Fluorescein was found to be quenched efficiently by iodide but not by acrylamide. The Stern–Volmer plot (Figure 3) is linear at low iodide concentration but has pronounced upward curvature at high iodide concentration, suggesting that additional quenching processes become operative at high concentration of iodide. The initial slope was used to calculate the quenching constant. A quenching constant of 5.4 M^{-1} for tRNA^{fMet}(3′-Flc) was obtained as compared to 6.9 M^{-1} for free fluorescein, suggesting that fluorescein in tRNA^{fMet}(3′-Flc) is highly accessible. As shown in Figure 3, the high accessibility of fluorescein in tRNA^{fMet} (3′-Flc) is drastically reduced upon binding of methionyl-tRNA synthetase. The binding of tRNA^{fMet} to methionyl-tRNA synthetase is weakened at high salt concentration, contributing to the upward curvature in the corresponding Stern–Volmer plot (Figure 3).

The rotational diffusion of fluorescein in tRNA^{fMet}(3′-Flc) was examined by steady-state emission anisotropy at 20 °C. The rotational relaxation time for the fluorescein residue in tRNA^{fMet}(3′-Flc) is 1.7 ns at 20 °C as determined from the Perrin plot (Figure 4). Since the rotational relaxation time for tRNA^{fMet} is 25 ns, the Perrin plot for tRNA^{fMet}(3′-Flc) clearly shows that the 3′-fluoresceinyl group has a high degree of local rotational freedom independent of the tRNA molecule. Upon binding of methionyl-tRNA synthetase, the anisotropy

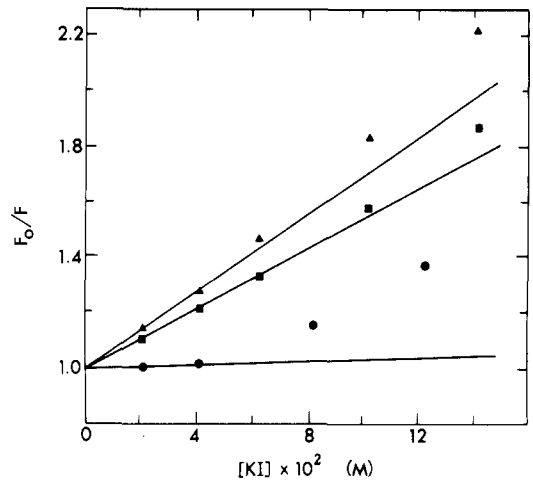

FIGURE 3: Stern–Volmer plots for the quenching of Flc (▲) and 3′-Flc emission by iodide. The iodide quenching data for 0.37 μM tRNA^{fMet}(3′-Flc) in the absence (■) and in the presence of 1.75 μM MetRS (●) are shown. The emission intensity at 520 nm (λ_{ex} at 480 nm) is measured in the presence of increasing concentration of KI relative to that of KCl. The slopes of the solid lines are used to estimate the Stern–Volmer collisional quenching constants for Flc in each system. The Stern–Volmer quenching constants are shown in Table II.

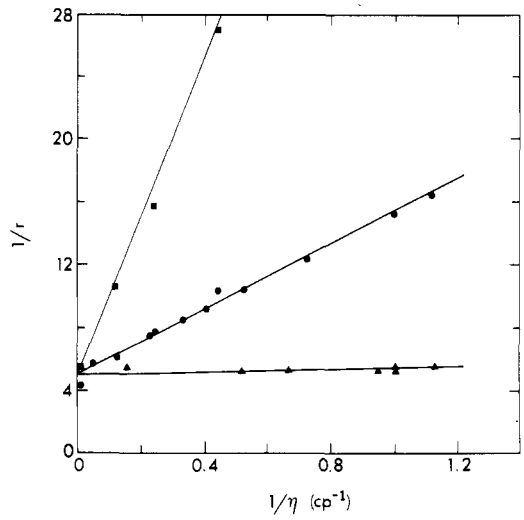

FIGURE 4: Perrin plots for Flc (■) and tRNA^{fMet}(3′-Flc) (●) at 20 °C. The viscosity, η, was varied by changing the concentration of sucrose in the sample. The anisotropy, r, was monitored at 520 nm. Also indicated is the 3′-Flc emission anisotropy for MetRS-bound tRNA^{fMet}(3′-Flc) (▲). The solid lines were used to determine the limiting anisotropy, r_0, and to calculate the rotational relaxation time, ϕ. The values of r_0 and ϕ are in Table II.

of the fluorescein group in tRNA^{fMet} (3′-Flc) is increased from 0.062 to 0.197 (Figure 4), corresponding a rotational relaxation time greater than 30 ns. Due to the short lifetime of fluorescein, the actual rotational relaxation time of synthetase-bound tRNA^{fMet}(3′-Flc) may be much longer. Nevertheless, these results suggest that the fluorescein residue in tRNA^{fMet}(3′-Flc) becomes immobilized upon binding of methionyl-tRNA synthetase. The fluorescence properties of free and methionyl-tRNA synthetase bound tRNA^{fMet}(3′-Flc) are summarized in Table II.

Interaction of tRNA^{fMet}(3′-DNS) with Methionyl-tRNA Synthetase. tRNA^{fMet}(3′-DNS) quenches the intrinsic fluorescence of methionyl-tRNA synthetase to 46%, slightly lower than that of unmodified tRNA^{fMet} (48%). The apparent dissociation constant determined from the titration of intrinsic fluorescence is 0.41 μM, comparable to that of native tRNA^{fMet} (0.22 μM).

Table II: Fluorescence Properties of the Fluorophore in Free and Methionyl-tRNA Synthetase Bound $tRNA^{fMet}$(3′-Flc)

	Flc	$tRNA^{fMet}$-(3′-Flc)	$tRNA^{fMet}$-(3′-Flc)-MetRS
absorption wavelength maximum, λ_{max}^{abs} (nm)	493	493	nd
excitation wavelength maximum, λ_{max}^{ex} (nm)	493	493	498
emission wavelength maximum, λ_{max}^{em} (nm)[a]	518	518	523
relative emission intensity, F/F_0, at 520 nm (λ_{ex} = 480 nm)	nd	1.00	0.59[b]
relative emission intensity, F/F_0, at 520 nm (λ_{ex} = 290 nm)	nd	1.00	1.15[b]
emission lifetime, τ (ns)	4[c]	3.6[d]	3.6[d]
anisotropy, r	0.018	0.062	0.197
limiting anisotropy, r_0	0.204	0.204	0.204
rotational relaxation time, ϕ (ns)	0.37	1.7	>30
Stern–Volmer quenching constant, K_q (M^{-1})	6.9	5.4	0.35
bimolecular quenching constant, k_q (M^{-1} ns^{-1})	1.7	1.5	0.10

[a] Corrected for the wavelength dependence of the sensitivity of the fluorometer detection system. [b] Determined from the titration of $tRNA^{fMet}$(3′-Flc) with methionyl-tRNA synthetase. [c] Birks et al., 1970. [d] Measured as described under Materials and Methods.

Table III: Fluorescence Properties of the Fluorophore in Free and Methionyl-tRNA Synthetase Bound $tRNA^{fMet}$(3′-DNS)

	DNS	$tRNA^{fMet}$-(3′-DNS)	$tRNA^{fMet}$-(3′-DNS)-MetRS
excitation wavelength maximum, λ_{max}^{ex} (nm)	322	326	332
emission wavelength maximum, λ_{max}^{em} (nm)[a]	520 (490)	550 (505)	530 (495)
relative emission intensity, F/F_0, at 510 nm (λ_{ex} = 340 nm)	nd	1.00	2.10[b]
emission lifetime, τ (ns)	nd	11	14
anisotropy, r	0.005	0.025	0.160
Stern–Volmer quenching constant, K_q (M^{-1})	20	6.3	2.3
bimolecular quenching constant, k_q (M^{-1} ns^{-1})	1.8	0.57	0.16

[a] λ_{max}^{em} values have been corrected for the wavelength dependence of the sensitivity of the detection system; the values in parentheses are uncorrected. [b] Determined from the titration of $tRNA^{fMet}$(3′-DNS) with MetRS.

As shown in Table III, the DNS emission in $tRNA^{fMet}$-(3′-DNS) is enhanced 110% in the presence of an excessive amount of methionyl-tRNA synthetase with a concomitant blue shift of 20 nm of the emission maximum and a 6-nm red shift in the excitation maximum. The emission lifetime also increased from 11 to 14 ns. The emission of DNS is known to be sensitive to the polarity of the local environment. These results are consistent with DNS in $tRNA^{fMet}$(3′-DNS) being localized in a relatively nonpolar environment upon binding of methionyl-tRNA synthetase. The fluorescence enhancement was utilized to obtain the binding parameters of $tRNA^{fMet}$ to methionyl-tRNA synthetase. The Scatchard plot of the fluorescence titration (data not shown) indicates that the stoichiometry for the binding site with a dissociation constant of 0.1 μM is close to 1 for dimeric methionyl-tRNA synthetase.

The solvent accessibility of DNS in $tRNA^{fMet}$(3′-DNS) is analyzed with acrylamide as the fluorescence quencher (Lehrer & Leavis, 1978). If both the emission intensity and the emission lifetime of dansylhydrazide are monitored at increasing concentration of acrylamide, the Stern–Volmer plot

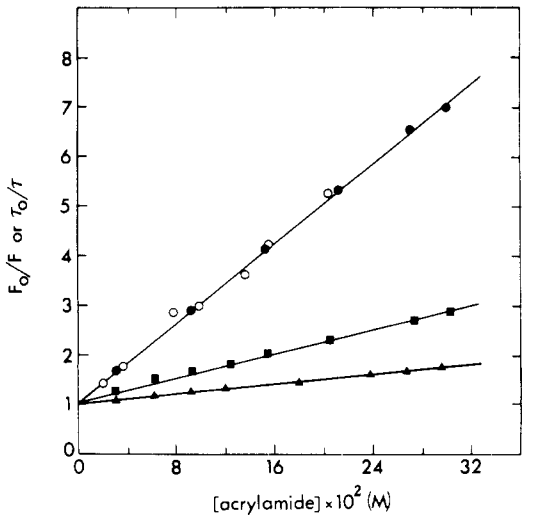

FIGURE 5: Stern–Volmer plot for the acrylamide quenching of dansylhydrazine (○, ●) and for 0.65 μM $tRNA^{fMet}$(3′-DNS) free in solution (■) and in the presence of 2.3 μM MetRS (▲). The data shown are all steady-state intensity measurements except data for dansyl hydrazine (○), which were obtained by fluorescence lifetime measurements. The Stern–Volmer quenching constants were determined from the slope of the solid lines and are given in Table III.

shows overlapping linear lines (Figure 5), indicating that dynamic quenching dominates the quenching process. The quenching constant of the fluorophore in $tRNA^{fMet}$(3′-DNS) was determined and compared to that for the $tRNA^{fMet}$(3′-DNS)–methionyl-tRNA synthetase complex (Figure 5). As shown in Table III, the collisional quenching rate constant of DNS is reduced by 3.6-fold when $tRNA^{fMet}$(3′-DNS) complexes with methionyl-tRNA synthetase. These results suggest that DNS in $tRNA^{fMet}$(3′-DNS) become less accessible or partially buried upon binding of methionyl-tRNA synthetase.

The steady-state anisotropy of the fluorophore in $tRNA^{fMet}$(3′-DNS) was found to be 0.025 (Table III). The anisotropy of the fluorophore increases to 0.16, when $tRNA^{fMet}$(3′-DNS) complexes with methionyl-tRNA synthetase, suggesting immobilization of the 3′-terminus after binding. Due to the heterogeneity of the limiting anisotropy of DNS with excitation and emission wavelengths (Hudson & Weber, 1974) and the corresponding lifetimes, the anisotropy measurements cannot be directly compared in terms of the rotational relaxation time. Attempts to experimentally determine the limiting anisotropy for the tRNA–synthetase complex with $tRNA^{fMet}$(3′-DNS) were unsuccessful.

Interaction of $tRNA^{fMet}$(D-PF) with Methionyl-tRNA Synthetase. $tRNA^{fMet}$(D-PF) binds to methionyl-tRNA synthetase with an apparent binding constant of 0.31 μM, as estimated from the quenching of methionyl-tRNA synthetase tryptophan emission.

The fluorescence properties of the fluorophore in free and methionyl-tRNA synthetase bound $tRNA^{fMet}$(D-PF) are summarized in Table IV. Upon binding to methionyl-tRNA synthetase, the proflavin fluorescence intensity was enhanced 10% without any other changes in the excitation or emission spectra. The steady-state emission anisotropy of proflavin in $tRNA^{fMet}$(D-PF) increased from 0.232 to 0.268 with a limiting anisotropy of 0.290 as determined from the Perrin plot (Figure 6). The corresponding rotational relaxation time increased from 21 to 65 ns with the emission lifetime of 5.2 ns. The accessibility of proflavin is studied with iodide as a collisional quencher. The Stern–Volmer plot for iodide quenching (Figure 7) is linear up to 0.2 M iodide. The accessibility of proflavin in $tRNA^{fMet}$(D-PF) is slightly increased upon binding

Table IV: Fluorescence Properties of the Fluorophore in Free and Methionyl-tRNA Synthetase Bound tRNA^{fMet}(D-PF)

	PF	tRNA^{fMet}-(D-PF)	tRNA^{fMet}-(D-PF)-MetRS
absorption wavelength maximum, λ_{max}^{abs} (nm)	444	462	nd
excitation wavelength maximum, λ_{max}^{ex} (nm)	443	462	462
emission wavelength maximum, λ_{max}^{em} (nm)[a]	512	510	510
relative emission intensity, F/F_0, at 500 nm (λ_{ex} = 455 nm)	nd	1.00	1.09[b]
relative emission intensity, F/F_0, at 500 nm (λ_{ex} = 290 nm)	nd	1.00	1.10[b]
emission lifetime, τ (ns)	5.0[c]	5.2[d]	5.2[d]
anisotropy, r	0.005	0.232	0.268
limiting anisotropy, r_0	0.067	0.290	0.290
rotational relaxation time, ϕ (ns)	0.40	21	65
Stern–Volmer quenching constant, K_q (M^{-1})	79	3.1	3.9
bimolecular quenching constant, k_q (M^{-1} ns^{-1})	16	0.60	0.75

[a] Corrected for the wavelength dependence of the sensitivity of the fluorometer detection system. [b] Determined from the titration of tRNA^{fMet}(3′-PF) with methionyl-tRNA synthetase. [c] Odom et al., 1979. [d] Measured as described under Materials and Methods.

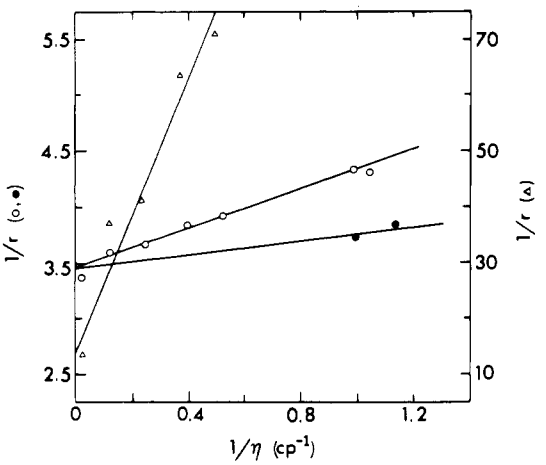

FIGURE 6: Perrin plot for PF (△) and tRNA^{fMet}(D-PF) (○), at 20 °C. The steady-state emission anisotropy, r, was monitored at 500 nm (λ_{ex} = 455 nm). The viscosity, η, was varied by changing the sucrose concentration of the sample. The emission anisotropy of MetRS-bound tRNA^{fMet}(D-PF) is also indicated (○). The solid lines were used to determine the limiting anisotropy, r_0, and the slopes were used to calculate rotational relaxation times, ϕ. The values of r_0 and ϕ, determined from this plot, are given in Table IV.

of methionyl-tRNA synthetase, as demonstrated by the slight increase of the bimolecular quenching rate constants (Table IV).

Interaction of tRNA^{fMet}(D-Etd) with Methionyl-tRNA Synthetase. tRNA^{fMet}(D-Etd) binds to methionyl-tRNA synthetase with an apparent dissociation constant of 0.4 μM, as estimated from the protein intrinsic fluorescence quenching.

Ethidium excitation maxima are blue-shifted and the emission maximum is red-shifted slightly when tRNA^{fMet}(D-Etd) complexes with methionyl-tRNA synthetase (Table V). In addition, the emission intensity of ethidium at 600 nm is reduced by 4%, similar to the case of phenylalanyl-tRNA synthetase (Ehrenberg et al., 1979). The anisotropy of ethidium emission in tRNA^{fMet}(D-Etd) increased from 0.196 to 0.250 upon binding of methionyl-tRNA synthetase; corresponding rotational relaxation times are 26 and 80 ns (Table V), respectively, using a weighted average lifetime of 12 ns and a limiting anisotropy of 0.287. It appears that ethidium

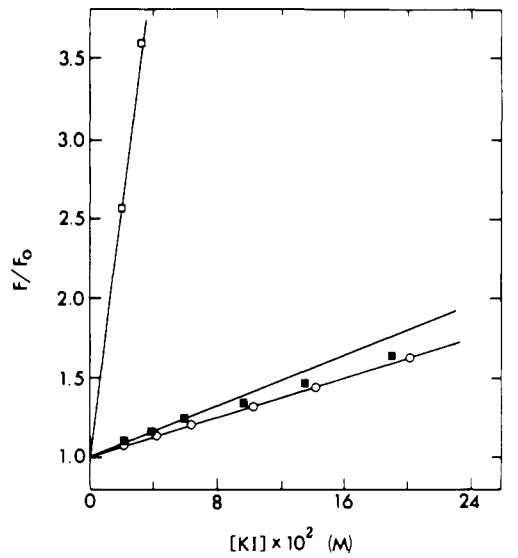

FIGURE 7: Stern–Volmer plot for the iodide quenching of PF (□) and for 0.37 μM tRNA^{fMet}(D-PF) free in solution (○) and in the presence of 1.6 μM MetRS (■). The emission intensity was monitored at 500 nm. F is the emission intensity of the sample in the presence of a given concentration of KI, and F_0 is the emission intensity of an identical sample except KCl is substituted for KI. The Stern–Volmer quenching constants, K_q, were determined from the slopes of the solid lines and are shown in Table IV.

Table V: Fluorescence Properties of the Fluorophore in Free and Methionyl-tRNA Synthetase Bound tRNA^{fMet}(D-Etd)

	ethidium	tRNA^{fMet}-(D-Etd)	tRNA^{fMet}-(D-Etd)-MetRS
absorption wavelength maximum, λ_{max}^{abs} (nm)	285, 480	305, 515	nd
excitation wavelength maximum, λ_{max}^{ex} (nm)	285, 480	305, 515	303, 510
emission wavelength maximum, λ_{max}^{em} (nm)[a]	615 (632)	596	600
relative emission intensity, F/F_0, at 600 nm (λ_{ex} = 520 nm)	0.07	1.00	0.96[b]
relative emission intensity, F/F_0, at 600 nm (λ_{ex} = 290 nm)	nd	1.00	0.96[b]
emission lifetime			
A_1, τ_1 (ns)	1.0, 1.8	0.69, 6.8	nd
A_2, τ_2 (ns)	nd	0.31, 24	nd
weighted arithmetic mean lifetime, $\langle\tau\rangle$ (ns)[c]	1.8	12	12
anisotropy, r	0.017	0.196	0.250
limiting anisotropy, r_0	0.130	0.287	(0.287)
rotational relaxation time, ϕ (ns)	0.27	26	80
relative quantum yield in H_2O and D_2O	3.7	1.9	1.9

[a] Not corrected for the wavelength dependence of the sensitivity of the fluorometer detection system. The value in parentheses is the corrected value (Wintermeyer & Zachau, 1979). [b] Determined from the titration of tRNA^{fMet}(D-EB) with MetRS. [c] Calculated according to $\langle\tau\rangle = \sum A_i\tau_i$.

in tRNA^{fMet}(D-Etd) is rigidly attached to tRNA and remains immobilized upon binding of methionyl-tRNA synthetase.

The solvent accessibility of ethidium in tRNA^{fMet}(D-Etd) is estimated by determining the enhancement of Etd emission in H_2O relative to that in D_2O, since the primary quenching mechanism is by proton transfer (Olmsted & Kearns, 1977). The emission intensity of ethidium in tRNA^{fMet}(D-Etd) is enhanced by a factor of 1.9 in D_2O relative to that in H_2O. This enhancement factor was not detectably changed for tRNA^{fMet}(D-Etd) in the presence of excess methionyl-tRNA synthetase, suggesting that the solvent accessibility is virtually unchanged upon binding methionyl-tRNA synthetase.

Table VI: Fluorescence Properties of the Fluorophore in Free and Methionyl-tRNA Synthetase Bound $tRNA^{fMet}(8-13)$

	$tRNA^{fMet}$-(8–13)	$tRNA^{fMet}$-(8–13)-MetRS
absorption wavelength maximum, λ_{max}^{abs} (nm)	388	nd
excitation wavelength maximum, λ_{max}^{ex} (nm)	388	388
emission wavelength maximum, λ_{max}^{em} (nm)[a]	436	436
relative emission intensity, F/F_0, at 460 nm (λ_{ex} = 390 nm)	1.00	1.00[b]
relative emission intensity, F/F_0, at 460 nm (λ_{ex} = 290 nm)	1.00	1.37[b]
emission lifetime, τ (ns)	4.7[c]	nd
anisotropy, r	0.255	0.286
limiting anisotropy, r_0	0.305	0.305
rotational relaxation time, ϕ (ns)	24	75

[a] Corrected for the wavelength dependence of the sensitivity of the fluorometer detection system. [b] Determined from the titration of $tRNA^{fMet}(8-13)$ with MetRS. [c] Determined as described in the text.

Interaction of $tRNA^{fMet}(8-13)$ with Methionyl-tRNA Synthetase. $tRNA^{fMet}(8-13)$ can be aminoacylated to 1.4 nmol/A_{260} unit, approximately 95% of the native $tRNA^{fMet}$ methionine acceptor activity. $tRNA^{fMet}(8-13)$ also quenches the intrinsic fluorescence of methionyl-tRNA synthetase to 48%, identical with that of the native $tRNA^{fMet}$. The apparent dissociation constant for $tRNA^{fMet}(8-13)$ and methionyl-tRNA synthetase is 0.46 μM on the basis of the protein intrinsic fluorescence titration, which is about 2-fold of that of native $tRNA^{fMet}$.

The emission properties of the fluorophore in $tRNA^{fMet}(8-13)$ are not detectably changed after the addition of an excess amount of methionyl-tRNA synthetase (Table VI). Acrylamide or potassium iodide does not quench the fluorophore at all. However, the emission intensity of the $tRNA^{fMet}(8-13)$ is reduced 81% after pancreatic ribonuclease digestion, in accord with the suggestion that the emission intensity depends primarily on the microscopic viscosity of the cross-linked product (Thomas et al., 1978). The pancreatic digestion product of $tRNA^{fMet}(8-13)$ cannot be quenched by acrylamide or iodide either. The emission anisotropy for free $tRNA^{fMet}(8-13)$ is 0.255 and increased to 0.286 upon binding of methionyl-tRNA synthetase. The limiting anisotropy of $tRNA^{fMet}(8-13)$ is 0.305. The emission lifetime of the fluorophore is 4.7 ns. The calculated rotational relaxation time for the fluorophore in $tRNA^{fMet}(8-13)$ is 24 ns and for the tRNA–synthetase complex is about 75 ns, assumming no changes in the limiting anisotropy or the lifetime of the fluorophore. These results suggest that the fluorophore in $tRNA^{fMet}(8-13)$ remains immobilized upon binding of methionyl-tRNA synthetase.

Singlet–Singlet Energy Transfer between Methionyl-tRNA Synthetase and Modified $tRNA^{fMet}$. Upon binding of methionyl-tRNA synthetase, the excitation spectra of some of the fluorophores in the modified tRNA are noticeably changed near 290 nm as a new maximum or a shoulder. As illustrated in Figure 8, the excitation spectra of $tRNA^{fMet}$(3′-DNS) in the presence of methionyl-tRNA synthetase shows a new peak. These changes are attributed to the singlet–singlet energy transfer between the intrinsic tryptophan fluorescence of methionyl-tRNA synthetase and the covalently attached fluorophore in modified tRNAs. The energy-transfer efficiency between tryptophan residues in methionyl-tRNA synthetase and each of the fluorophores in modified tRNA's can be experimentally determined from the sensitized emission. The emission intensity at the emission maximum by excitation at 290 nm is measured for each of the modified tRNA's at increasing concentration of methionyl-tRNA synthetase

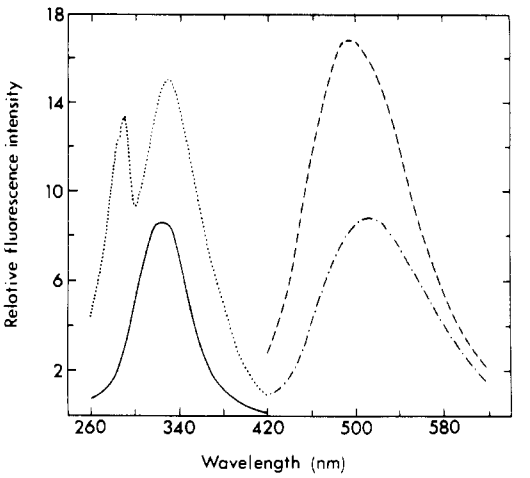

FIGURE 8: Fluorescence excitation (—, ···) and emission (–·–, – –) spectra for 1.3 μM $tRNA^{fMet}$(3′-DNS) free in solution (—, –·–) and in the presence of 1.92 μM MetRS (···, – –). The excitation and emission spectra were recorded with the emission monochromator set at 510 nm and the excitation monochromator set at 340 nm, respectively.

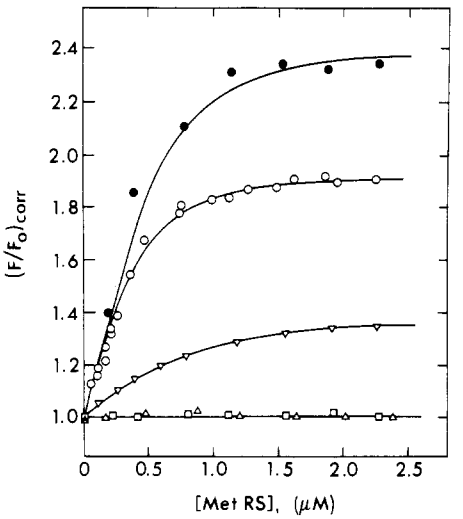

FIGURE 9: Fluorescence titration of 1.3 μM $tRNA^{fMet}$(3′-DNS) (●), 1.3 μM $tRNA^{fMet}(8-13)$ (▽), 0.92 μM $tRNA^{fMet}$(D-EB) (□), 0.39 μM $tRNA^{fMet}$(D-PF) (△), and 0.37 μM $tRNA^{fMet}$(3′-Flc) (○) with methionyl-tRNA synthetase. The relative emission intensity, F/F_0, was monitored at λ_{ex} = 290 nm, and λ_{em} was 510, 460, 600, 500, and 520 nm for the 3′-DNS-, 8–13-, D-EB-, D-PF-, and 3′-Flc-modified $tRNA^{fMet}$'s, respectively. The emission contribution of enzyme was subtracted. The emission intensity has been corrected for the change in emission intensity of directly excited fluorophore with increasing methionyl-tRNA synthetase concentration, as described in the text.

(Figure 9). Corrections were made for the changes in the fluorescence intensity of directly excited fluorophore due to the change of the local environment upon binding of methionyl-tRNA synthetase. As shown in Figure 9, energy transfer evidently occurs when $tRNA^{fMet}$(3′-Flc), $tRNA^{fMet}$(3′-DNS), and $tRNA^{fMet}(8-13)$ were bound but not when $tRNA^{fMet}$(D-PF) and $tRNA^{fMet}$(D-Etd) were bound. These results suggest that the dihydrouracil loop (D loop) in $tRNA^{fMet}$ is likely located farther away from methionyl-tRNA synthetase in comparison to the 3′-terminus or S8–C13, since the two different fluorophores attached at the same location in the D-loop in $tRNA^{fMet}$ did not show detectable energy transfer. Unfortunately, the transfer efficiency determined in these cases, where energy transfer does occur, cannot be directly interpreted in terms of the apparent distances between the fluorophores and the tryptophan residues in methionyl-tRNA

synthetase, due to the presence of multiple donors (27 tryptophan residues in methionyl-tRNA synthetase) with unknown spatial distribution, orientation, mobility, and quantum yield.

Discussion

In the present investigation, the conformations of tRNA^{fMet} and methionyl-tRNA synthetase bound tRNA^{fMet} are analyzed with tRNA^{fMet} labeled with a single fluorophore. Five species of tRNA^{fMet} modified at the 3′-end, dihydrouridine, and thiouridine were used. The methionyl-tRNA synthetase binding affinity for each of the modified tRNA^{fMet}'s was the same as or reduced by only a small degree relative to that for unmodified tRNA^{fMet}. Each of the labeled tRNA^{fMet}'s was shown to induce close to the same extent of methionyl-tRNA synthetase tryptophan quenching as unmodified tRNA^{fMet}. The 3′-labeled tRNA^{fMet}'s were shown to bind to a single high-affinity site on methionyl-tRNA synthetase, as monitored by the change in the emission intensity of the probe localized at the 3′-terminus of tRNA^{fMet}. These results show that the interaction of the fluorescent-labeled tRNA^{fMet} with methionyl-tRNA synthetase is very similar to that of unmodified tRNA^{fMet}. The conclusions drawn from the present study may be reasonably extended to the interaction between unmodified tRNA^{fMet} and methionyl-tRNA synthetase.

Fluorescence Properties at the 3′-Terminus. The changes of the emission properties, including spectral shift and quantum yield for the fluorophores at the 3′-terminus (DNS and fluorescein), are consistent with an increase in the hydrophobicity in the local environments of these probes. DNS is known to show high quantum yield and blue-shift, while fluorescein shows spectral red-shift in a nonpolar environment.

The conformational changes at the 3′-end are also demonstrated by the changes in the accessibility and anisotropy. Both DNS in tRNA^{fMet}(3′-DNS) and fluorescein in tRNA^{fMet}-(3′-Flc) showed a drastic decrease in accessibility and increase in anisotropy upon binding of methionyl-tRNA synthetase. The fluorescein group in tRNA^{fMet}(3′-Flc) appears to be more mobile and more accessible than DNS in tRNA^{fMet}(3′-DNS). The differences may be due to the different spacer groups linking tRNA and the fluorophore. No changes in the fluorescence properties of the fluorophores at the 3′-terminus were observed when tRNA^{Phe}(3′-Flc), tRNA^{Phe}(3′-DNS), or tRNA^{Glu}(3′-Flc) were used.

Conformational States at the 3′-Terminus. In the crystal structure for tRNA^{fMet}, the arm formed by the last five unpaired nucleotides at the 3′-terminus curls back toward the acceptor stem (Woo et al., 1980). In contrast, in the crystal structure of yeast tRNA^{Phe}, the last five nucleotides at the 3′-terminus are extended and continue the helical organization of the acceptor stem (Kim et al., 1974; Robertus et al., 1974). Fluorescence anisotropy measurements suggest that the 3′-termini of both tRNA^{fMet} and yeast tRNA^{Phe} are flexible with local rotational freedom independent of the rest of the tRNA molecule. This result indicates that in solution at 20 °C several different conformations of the 3′-terminus of the tRNA may be possible. It is reasonable that the conformations of the 3′-termini in the crystal structures of *E. coli* tRNA^{fMet} and yeast tRNA^{Phe} represent two possible conformations, of similar stability, which may exist in solution. When tRNA^{fMet} binds to methionyl-tRNA synthetase, essentially a single conformation of the 3′-terminus is stabilized by interactions of tRNA with methionyl-tRNA synthetase. The results of the present study suggest that methionyl-tRNA synthetase induces a conformational change and selects a specific conformation of the 3′-terminus of tRNA^{fMet}, when tRNA complexes with the synthetase. The conformational change detected by the 3′-fluorophores likely reflects the correct positioning of the 3′-terminus of tRNA^{fMet} in the active site of methionyl-tRNA synthetase. However, the possible involvement of the fluorophores in the observed effects cannot be excluded.

Nucleotide Binding Fold and 3′-Terminus Binding Site. The observed changes at the 3′-terminus can be attributed to either a direct interaction of the 3′-terminus with synthetase or conformational changes at the 3′-terminus of tRNA^{fMet} upon binding of methionyl-tRNA synthetase. These two possibilities are not mutually exclusive. In either case, the fluorescent groups at the 3′-terminus are likely surrounded by a hydrophobic pocket on the surface of the protein molecule near the active site of methionyl-tRNA synthetase. It is tempting to speculate that the hydrophobic pocket is related to the nucleotide binding fold (Rossmann fold) observed in the crystal structure of trypsin-modified methionyl-tRNA synthetase (Risler et al., 1981). The nucleotide binding fold has been shown to be the binding site of 8-Br-ATP (Risler et al., 1981). Cibacron F3GA is known to bind to the nucleotide binding fold (Beissner et al., 1979).

We envision that Cibacron F3GA mimics the orientation of the aromatic rings and anionic groups of ATP and nucleotides at the 3′-terminus of tRNA^{fMet} in binding to methionyl-tRNA synthetase. The hydrophobic site on methionyl-tRNA synthetase detected by the fluorophores at the 3′-terminus of tRNA^{fMet} overlaps with the Cibacron F3GA binding site, as hydrophobic interactions are known to be very important in its binding of proteins (Beissner et al., 1979). This interpretation is consistent with the proposal that the 3′-terminal nucleotides are critical in triggering the conformational adaptation between the synthetase and its cognate tRNA (von der Haar & Gaertner, 1975; Krauss et al., 1977). It follows that the conformational changes at the 3′-terminus of tRNA^{fMet}, detected by the fluorophores in the present investigation, are critical in triggering the recognition processes between tRNA^{fMet} and methionyl-tRNA synthetase.

It is interesting to note that the hydrophobic site on methionyl-tRNA synthetase cannot be detected with free fluorophores such as anilinonaphthalenesulfonate in the presence or in the absence of tRNA^{fMet} (B. Q. Ferguson and D. C. H. Yang, unpublished results), although anilinonaphthalenesulfonate is known to be highly sensitive for detecting hydrophobic pockets (Stryer, 1965). It is likely that the hydrophobic site, detected by the fluorophores at the 3′-terminus of tRNA^{fMet}, is formed in methionyl-tRNA synthetase after the binding of tRNA^{fMet}, which also blocks the access of anilinonaphthalenesulfonate.

Conformational States at the D Loop and 8–13. The emission properties of tRNA^{fMet}(D-PF) resemble those of intercalated PF in complex with DNA or RNA (Georghiou, 1975; Schreiber & Daune, 1974). In tRNA^{fMet}, D20 is located between G19 and A21. Since the partial quenching of PF fluorescence in tRNA^{fMet} relative to free PF resembles its binding of GMP or intercalation in a G-C pair rather than an A-T pair (Schreiber & Daune, 1974), the present results suggest that PF is stacked over G19 rather than A21. The restricted rotational freedom of PF in tRNA^{fMet}(D-PF) is consistent with such stacked structure.

Upon binding of methionyl-tRNA synthetase, there is a slight increase in emission intensity of PF and in solvent accessibility. This can be best interpreted as partial unstacking of proflavin from G19.

The emission properties of tRNA^{fMet}(D-Etd) resemble those of intercalated ethidium in tRNA (Olmsted & Kearn, 1977) or DNA. The anisotropy measurements suggest that ethidium

at D20 is immobile relative to the entire tRNA molecule. Since the primary quenching mechanism for ethidium is proton transfer, the observed emission properties are not indicative of the polarity of the surroundings of ethidium. Nonetheless, small changes of the fluorescence properties in $tRNA^{fMet}$(D-Etd) were observed upon binding of methionyl-tRNA synthetase, which is consistent with a subtle conformational change at the D loop of $tRNA^{fMet}$. Whether such changes occur in the unmodified tRNA is yet to be further analyzed.

No fluorescence change was observed in $tRNA^{fMet}$(8–13) upon binding of methionyl-tRNA synthetase. The S8–C13 photo-cross-link product is known to be sensitive primarily to the local viscosity (Thomas et al., 1978). Anisotropy measurement indicates that S8–C13 is immobile relative to the tRNA molecule. Thus, the undetectable change in $tRNA^{fMet}$(8–13) does not necessarily suggest that the conformation does not change at this location. It should be noted that the rate constant of photo-cross-linking in $tRNA^{Phe}$ is decreased upon binding of phenylalanyl-tRNA synthetase and that modified tRNA shows lower affinity toward the enzyme (Holler et al., 1981). Schimmel and co-workers (Starzyk, 1982) have proposed a covalent intermediate at this location with the synthetase.

Rotational Freedom of tRNA–Synthetase Complex. The observed rotational relaxations times are 65–80 ns for methionyl-tRNA synthetase bound-$tRNA^{fMet}$, as determined from the fluorophore attached to the tRNA molecule. The predicted rotational relaxation time for the tRNA–synthetase complex is at least 85–100 ns, depending on the axial ratio of the equivalent ellipsoid of methionyl-tRNA synthetase. Since some of the fluorophores in modified $tRNA^{fMet}$ are shown to be immobile, these results are compatible with the presence of a flexible linkage between the two subunits or different structural domains in methionyl-tRNA synthetase. More thorough studies on this aspect will be reported later with fluorescent-labeled methionyl-tRNA synthetase.

Energy Transfer and Relative Orientation of tRNA and Synthetase. The transfer efficiency for multidonor–single acceptor energy-transfer measurement depends on the sizes and the shapes of the donors, the orientation and mobility of the donor's emission dipoles and acceptor's absorption dipoles, and the separation vectors between donors and the acceptor. In the present case, the number of fluorescent tryptophan residues and the extent of intertryptophanyl energy transfer are not known. The large number of tryptophan residues (Cassio & Waller, 1974) in methionyl-tRNA synthetase further complicated the interpretation of the energy-transfer measurements. A normalized transfer efficiency is calculated by assuming that all energy transfer originates from a single fluorescent tryptophan residue. The normalized energy-transfer efficiency was obtained by multiplying the observed efficiency with the total number of tryptophan residues in methionyl-tRNA synthetase. Apparent distances were then calculated according to eq 5. The resulting apparent distances suggest that the 3′-terminus and S8–C13 are about 20 Å closer to the hypothetical tryptophan residue than D20. Such an orientation is qualitatively in agreement with that synthetase is binding at the inner loop of an L-shaped tRNA molecule (Rich & Schimmel, 1977).

Delocalized Conformational Changes. The energy-transfer measurements do not give any indication that the D loop of $tRNA^{fMet}$ interacts directly with either subunit of the methionyl-tRNA synthetase dimer, when $tRNA^{fMet}$ binds at a single site on the dimeric enzyme. These results are consistent with previous studies involving $tRNA^{fMet}$ fragments (Seno et al., 1969), chemically modified $tRNA^{fMet}$ (Schulman & Pelka, 1977), photochemical cross-linking of $tRNA^{fMet}$ to methionyl-tRNA synthetase (Rosa et al., 1979), and the protection of $tRNA^{fMet}$ by methionyl-tRNA synthetase, from ribonuclease digestion (Dube, 1973).

The methionyl-tRNA synthetase induced changes in the fluorescence of probes located at the D20 position of $tRNA^{fMet}$ apparently are not resulted from direct interactions of the probe with methionyl-tRNA synthetase. This result indicates that methionyl-tRNA synthetase can induce a small, but significant delocalized conformational change in $tRNA^{fMet}$ transmitted to the D loop from other parts of the tRNA molecule interacting with the enzyme. This result supports the hypothesis that the tRNA molecule is conformationally flexible (Harvey & McCammon, 1981; Ehrenberg et al., 1979; Robertson & Wintermeyer, 1981). However, the extent of conformational changes cannot be determined as to the angular movement of the helixes. We have carried out a series of energy-transfer experiments using $tRNA^{fMet}$ bearing both donor and acceptor groups. Comparison of the transfer efficiency of the free and synthetase-bound tRNA gave more defined conformational constraints. The present studies will be necessary for normalizing and interpreting the results of energy-transfer experiments. Since the crystal structures of $tRNA^{fMet}$ and methionyl-tRNA synthetase are known, it may be possible then to formulate a model for the tRNA–synthetase complex on the basis of the results of fluorescence and other studies.

The methodology developed and applied in this study may be extended to the study of other tRNA-synthetase systems, protein factors, or ribosomes. Further studies by relaxation kinetics may elucidate the mechanism of the conformational transitions in $tRNA^{fMet}$. The conclusions drawn may be general for tRNA–synthetase interactions. Further studies on the solution structure of the tRNA synthetase complex should be useful for our understanding of protein–nucleic acid interaction in general.

Registry No. MetRS, 9033-22-1.

REFERENCES

Ackerman, E. J., Joachimiak, A., Klinghofer, V., & Sigler, P. (1985) *Cell (Cambridge, Mass.) 181*, 93–102.

Barker, D. G., Ebel, J. P., Jakes, R., & Bruton, C. J. (1982) *Eur. J. Biochem. 127*, 449–459.

Beissner, R. S., Quiocho, F. A., & Rudolph, F. B. (1979) *J. Mol. Biol. 134*, 851–853.

Berman, H. A., Yguerabide, J., & Taylor, P. (1980) *Biochemistry 19*, 2226–2235.

Birks, J. B. (1970) *Photophysics of Aromatic Molecules*, Wiley-Interscience, New York.

Blanquet, S., Iwatsubo, M., & Waller, J. P. (1973) *Eur. J. Biochem. 36*, 213–226.

Blanquet, S., Dessen, P., & Fayat, G. (1979) in *Transfer RNA: Structure, Properties and Recognition* (Abelson, J., Schimmel, P., & Soll, D., Eds.) pp 281–299, Cold Spring Harbor Laboratory, Cold Spring Harbor, NY.

Bohme, H. J., Kopperschlager, G., Schulz, J., & Hofmann, E. (1972) *J. Chromatogr. 69*, 209–214.

Bruton, C. J., & Hartley, B. S. (1970) *J. Mol. Biol. 52*, 165–178.

Cantley, L. C., & Hammes, G. G. (1976) *Biochemistry 15*, 1–14.

Cantor, C. R., & Tao, T. (1971) *Procedures in Nucleic Acid Research* (Cantoni, G. C., & Davies, D. R., Eds.) Vol. 2, pp 31–93, Harper and Row, New York.

Cassio, D., & Waller, J.-P. (1974) *Eur. J. Biochem. 20*, 283–300.
Crothers, D. W., Cole, P. E., Hiblers, C. W., & Shulman, R. G. (1974) *J. Mol. Biol. 87*, 63–68.
Dale, R. E., & Eisinger, J. (1975) *Biochemical Fluorescence: Concepts* (Chen R. F., & Edelhoch, H., Eds.) Vol. I, pp 115–284, Marcel Dekker, New York.
Dessen, P., Fayat, G., Zaccai, G., & Blanquet S. (1982) *J. Mol. Biol. 154*, 603–613.
Dube, S. K. (1973) *Nature (London), New Biol. 243*, 103–105.
Eftink, M. R., & Ghiron, A. (1977) *Biochemistry 16*, 5546–5551.
Ehrenberg, M., Rigler, R., & Wintermeyer, W. (1979) *Biochemistry 18*, 4588–4599.
Engel, G. (1974) *Anal. Biochem. 61*, 184–191.
Fairclough, R. H., & Cantor, C. R. (1978) *Methods Enzymol. 48*, 347–379.
Fairclough, R. H., & Cantor, C. R. (1979) *J. Mol. Biol. 132*, 575–586.
Fasman, G., Ed. (1975) *Handbook of Biochemistry and Molecular Biology*, 3rd ed., Vol. 1, CRC Press, Cleveland, OH.
Favre, A., Michelson, A. M., & Yaniv, M. (1971) *J. Mol. Biol. 58*, 367–379.
Ferguson, B. Q., & Yang, D. C. H. (1981) *Fed. Proc., Fed. Am. Soc. Exp. Biol. 40*, 1807.
Forster, T. (1966) in *Modern Quantum Chemistry* (Sinanoglu, O., Ed.) Section III, pp 93–137, Academic Press, New York.
Georghiou, S. (1975) *Photochem. Photobiol. 22*, 103–109.
Haas, E., Katzir, E. K., & Steinberg, I. Z. (1978) *Biochemistry 17*, 5064–5070.
Harvey, S. C., & McCammon, J. A. (1981) *Nature (London) 294*, 286–287.
Heinrikson, R. L., & Hartley, B. S. (1967) *Biochem. J. 105*, 17–24.
Hillel, Z., & Wu, C. W. (1976) *Biochemistry 15*, 2105–2113.
Holler, E., Baltzinger, M., & Favre, A. (1981) *Biochemistry 20*, 1139–1147.
Hudson, E. N., & Weber, G. (1973) *Biochemistry 12*, 4154–4161.
Johnson, D. L., Dang, C. V., & Yang, D. C. H. (1979) *J. Biol. Chem. 255*, 4362–4366.
Kim, S. H., Suddath, F. L., Quigley, G. J., McPherson, A., Susmann, J. L., Wang, A., Seeman, N. C., & Rich, A. (1974) *Science (Washington, D.C.) 185*, 435–440.
Klotz, I. M., & Hunston, D. L. (1971) *Biochemistry 10*, 3065–3069.
Krauss, G., Riesner, D., & Maas, G. (1976) *Eur. J. Biochem. 68*, 81–93.
Laemmli, U. K. (1970) *Nature (London) 227*, 680–685.
Lehrer, S. S., & Leavis, P. C. (1978) *Methods Enzymol. 49*, 222–236.
Lemoine, F., Waller, J.-P., & van Rapenbusch, R. (1968) *Eur. J. Biochem. 4*, 213–221.
Martin, M. M., & Lindquist, L. (1973) *Chem. Phys. Lett. 22*, 309–312.
Mercola, D. A., Morris, J. W. S., & Arquilla, R. (1972) *Biochemistry 11*, 3860–3874.
Odom, O. W., Robbins, D. J., Lynch, J., Dottavio-Martin, D., Kramer, G., & Hardesty, B. (1980) *Biochemistry 19*, 5947–5954.
Olmsted, J., & Kearns, D. R. (1977) *Biochemistry 16*, 3647–3654.
Pachmann, U., Cronvall, E., Rigler, R., Hirsch, R., Wintermeyer, W., & Zachau, H. G. (1973) *Eur. J. Biochem. 39*, 265–273.
Rich, A., & Schimmel, P. R. (1977) *Nucleic Acids Res. 4*, 1649–1665.
Risler, J. L., Zelwer, C., & Brunet, S. (1981) *Nature (London) 292*, 384–386.
Robertson, J. M., & Wintermeyer, W. (1981) *J. Mol. Biol. 151*, 57–79.
Robertus, J. D., Ladner, J. E., Finch, J. T., Rhodes, D., Brown, R. S., Clark, B. F. C., & Klug, A. (1974) *Nature (London) 250*, 546–551.
Rosa, J. J., Rosa, M. D., & Sigler, P. B. (1979) *Biochemistry 18*, 637–647.
Schimmel, P. R., & Söll, D. G. (1979) *Annu. Rev. Biochem. 48*, 601–648.
Schreiber, J. P., & Daune, M. P. (1974) *J. Mol. Biol. 83*, 487–501.
Schulman, L. H., & Pelka, H. (1977) *Biochemistry 16*, 4256–4265.
Schulman, L. H., Valenzuela, D., & Pelka, H. (1981) *Biochemistry 20*, 6018–6023.
Schulman, L. H., Pelka, H., & Susaui, M. (1983) *Nucleic Acids Res. 11*, 1439–1455.
Scott, T. G., Spencer, R. D., Leonard, N. J., & Weber G. (1970) *J. Am. Chem. Soc. 92*, 687–695.
Seno, T., Kobayashi, M., & Nishimura, S. (1969) *Biochim. Biophys. Acta 190*, 285–303.
Shinitzky, M. (1972) *J. Chem. Phys. 56*, 5979–5981.
Starzyk, R. M., Koontz, S. W., & Schimmel, P. R. (1982) *Nature (London) 298*, 136–140.
Stern, O., & Volmer, M. (1919) *Phys. Z. 20*, 183–188.
Stryer, L. (1965) *J. Mol. Biol. 13*, 482–495.
Thomas, G., Fourrey, J. L., & Favre, A. (1978) *Biochemistry 17*, 4500–4514.
Uemura, H., Imai, M., Ohtsuka, E., Ikahara, M., & Soll, D. (1982) *Nucleic Acids Res. 10*, 6531–6539.
Wahl, P. (1975) *Biochemical Fluorescence: Concepts* (Chen, R. F., & Edelhoch, H., Eds.) Vol. 1, pp 1–36, Marcel Dekker, New York.
Wells, B. D., & Cantor, C. R. (1977) *Nucleic Acids Res. 4*, 1668–1680.
Wells, B. D., & Cantor, C. R. (1980) *Nucleic Acids Res. 8*, 3229–3247.
Wintermeyer, W., & Zachau, H. G. (1979) *Eur. J. Biochem. 98*, 465–475.
Wintermeyer, W., Schleich, H. G., & Zachau, H. G. (1979) *Methods Enzymol. 59*, 110–121.
Woo, N. H., Roe, B. A., & Rich, A. (1980) *Nature (London) 286*, 346–351.
Wrede, P., Woo, N. H., & Rich, A. (1979) *Proc. Natl. Acad. Sci. U.S.A. 76*, 3289–3293.
Yang, C. H., & Söll, D. G. (1974) *Proc. Natl. Acad. Sci. U.S.A. 71*, 2838–2842.
Yguerabide, J. (1972) *Methods Enzymol. 26*, 498–578.
Zelwer, C., Risler, J. L., & Brunie, S. (1982) *J. Mol. Biol. 155*, 63–81.